Science in China Series D: Earth Sciences

www.scichina.com
earth.scichina.com
www.springerlink.com

High resolution aerosol optical thickness retrieval over the Pearl River Delta region with improved aerosol modelling

WONG ManSing[1], NICHOL Janet[1†], LEE Kwon Ho[2] & LI ZhanQing[2]

[1] Department of Land Surveying and Geo-Informatics, The Hong Kong Polytechnic University, Hong Kong, China;
[2] Earth System Science Interdisciplinary Center, University of Maryland (UMD), USA

Aerosol retrieval algorithms for the MODerate Resolution Imaging Spectroradiometer (MODIS) have been developed to estimate aerosol and microphysical properties of the atmosphere, which help to address aerosol climatic issues at global scale. However, higher spatial resolution aerosol products for urban areas have not been well researched mainly due to the difficulty of differentiating aerosols from bright surfaces in urban areas. Here, a new aerosol retrieval algorithm using the MODIS 500 m resolution images is described, to retrieve aerosol properties over Hong Kong and the Pearl River Delta region. The rationale of our technique is to first estimate the aerosol reflectance by decomposing the top-of-atmosphere reflectance from surface reflectance and Rayleigh path reflectance. For the determination of surface reflectance, a modified Minimum Reflectance Technique (MRT) is used, and MRT images are computed for different seasons. A strong correlation is shown between the surface reflectance of MRT images and MODIS land surface reflectance products (MOD09), with a value of 0.9. For conversion of aerosol reflectance to Aerosol Optical Thickness (AOT), comprehensive Look Up Tables (LUT) are constructed, in which aerosol properties and sun-viewing geometry in the radiative transfer calculations are taken into account. Four aerosol types, namely mixed urban, polluted urban, dust, and heavy pollution, were derived using cluster analysis on three years of AERONET measurements in Hong Kong. Their aerosol properties were input for LUT calculation. The resulting 500 m AOT images are highly correlated ($r = 0.89$) with AERONET sunphotometer observations in Hong Kong. This study demonstrates the applicability of aerosol retrieval at fine resolution scale in urban areas, which can assist the study of aerosol loading distribution and the impact of localized and transient pollution on urban air quality. In addition, the MODIS 500 m AOT images can be used to study cross-boundary aerosols and to locate pollutant sources in the Pearl River Delta region.

aerosol retrieval, aerosol optical thickness, AERONET, MODIS, satellite image

1 Introduction

Aerosol retrieval from remote sensing satellite images has been studied for three decades. The basic aim is to retrieve the spectral information about the atmosphere from the path between the surface and satellite. It is always complicated to retrieve aerosol because ground surface reflectance is difficult to distinguish from the total satellite received signal. The estimation of surface reflectance is then the key factor on the aerosol retrieval, which attempts to differentiate the aerosol signal from surface.

Kaufman and Tanré[1] first proposed the Dense Dark Vegetation (DDV) method using the multi-wavelength algorithm on the MODerate Resolution Imaging Spectroradiometer (MODIS) satellite images. The DDV al-

Received August 28, 2008; accepted May 13, 2009; published online July 25, 2009
doi: 10.1007/s11430-009-0125-9
†Corresponding author (email: lsjanet@polyu.edu.hk)
Supported by the Hong Kong CERG Grant (Grant No. PolyU 5253/07E)

Citation: Wong M S, Nichol J, Lee K H, et al. High resolution aerosol optical thickness retrieval over the Pearl River Delta region with improved aerosol modelling. Sci China Ser D-Earth Sci, 2009, 52(10): 1641-1649, doi: 10.1007/s11430-009-0125-9

gorithm (known as collection 4) works on different aerosol scattering properties loaded on different wavelengths (e.g., longer wavelength has smaller aerosol loading). The algorithm works only on pixels of vegetation areas with coverage larger than 60% but cannot operate over bright deserts and urban areas. Chu et al.[2] revealed that the MODIS collection 4 (DDV) algorithm had a positive bias in comparison to the AErosol Robotic NETwork (AERONET) sunphotometer data (Holben et al.[3]), and Remer et al.[4] and Levy et al.[5] reported certain inherent problems in determining surface reflectance using the DDV algorithm. Recently, Levy et al.[6] modified the surface reflectance determination in the MODIS aerosol retrieval algorithm (known as collection 5) by considering the band correlation based on vegetation index ($NDVI_{SWIR}$) and the scattering angle. The new collection 5 data has been evaluated (Mi et al.[7]) with significant improvements in both accuracy and continuity of the Aerosol Optical Thickness (AOT) in China. However, two major limitations remain of MOD04 data for local/urban scale study, namely bright surfaces such as urban areas, and low spatial resolution. To overcome these limitations, new techniques were developed in this study.

In order to infer the aerosol contents from surface reflectance, a surface reflectance database was developed based on the Minimum Reflectance Technique (MRT). This technique explains the lowest reflecting pixels over a time series of co-registered images and retains them to create the minimum reflectance image over time period. Herman and Celarier[8] used the MRT technique for TOMS data and Koelemeijer et al.[9] used it on GOME data. In view of the coarse resolution the accuracy of AOT (of within 30% of AERONET ground measurements) could be considered good. However, the 10 km spatial resolution of the MODIS products only provide meaningful depictions on a broad regional scale, whereas aerosol monitoring over complex regions, such as urban areas in Hong Kong SAR (1095 km^2) requires more spatial and spectral details. Li et al.[10] developed a 1 km AOT algorithm based on the MODIS collection 4 algorithm for a study in Hong Kong, but it was limited to dense vegetated areas; the validation was made using handheld sunphotometers over vegetated surfaces only and no validation was done over the urban areas. In order to retrieve and map aerosol loading distributions over urban areas at a high level of details, a new MODIS 500 m resolution aerosol retrieval algorithm was proposed in this study.

2 Study area and data used

Hong Kong, a commercial and financial city located in southeast China (Figure 1), has suffered serious air pollution for years. Its nearby the Pearl River Delta (PRD) region has been increasingly vulnerable to direct developments such as urbanization and industrial expansion. The cities of Hong Kong and Macau situated on opposite sides of the PRD are directly affected in their economy and activities by such changes. Ref. [11] showed that in the year 1997 emission inventory for volatile organic compounds (VOC), respiratory suspended particles (RSP), nitrogen oxides (NO_x), and sulphur dioxide (SO_2), the PRD region was the dominant source area for emissions with 88% of VOC, 95% of RSP, 80% of NO_x and 87% of SO_2 affecting Hong Kong.

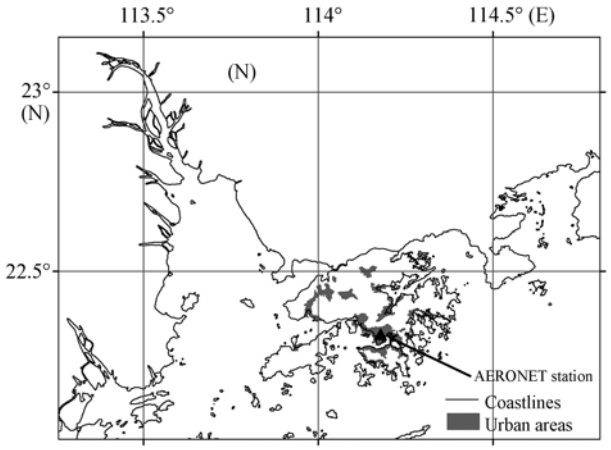

Figure 1 Map of Hong Kong and AERONET station.

In this project, the MODIS level 1B calibrated images (500 m) and MODIS level 2 aerosol products (MOD04) of year 2007 were acquired. The retrieved 500 m AOT images were validated with the data from the Hong Kong AERONET station. AERONET (Holben et al.[3]) is a global network of ground sunphotometers, which consists of a Cimel sunphotometer for measuring aerosol extinction every fifteen minutes using multiple wavelengths.

3 Methodology

The TERRA/MODIS 500 m resolution data (470, 550, 660 nm) was used for aerosol retrieval over the urban area for the year 2007. The rationale of the proposed

aerosol retrieval algorithm is to determine the aerosol reflectance by decomposing the Top-of-Atmosphere (TOA) reflectance from surface reflectance and the Rayleigh path reflectance. The aerosol reflectance ρ_{Aer} can be determined by eq. (1):

$$\rho_{\text{TOA}} = \rho_{\text{Aer}} + \rho_{\text{Ray}} + \frac{\Gamma_{\text{Tot}}(\theta_0) \cdot \Gamma_{\text{Tot}}(\theta_s) \cdot \rho_{\text{Surf}}}{1 - \rho_{\text{Surf}} \cdot r_{\text{Hem}}}, \quad (1)$$

where θ_0 is the solar zenith angle, θ_s is the satellite zenith angle, ρ_{Aer} is the aerosol reflectance, ρ_{Ray} is the Rayleigh reflectance, $\Gamma_{\text{Tot}}(\theta_0)$ is the transmittance along the path from the sun to ground, $\Gamma_{\text{Tot}}(\theta_s)$ is the transmittance along the path from the sensor to ground, ρ_{Surf} is the surface reflectance, and r_{Hem} is the hemispheric reflectance. Figure 2 illustrates the work flow of aerosol retrieval in this study.

In order to validate the surface reflectance estimated from MRT, the MODIS surface reflectance products (MOD09 8-days composite surface reflectance images) were also acquired from NASA Goddard Earth Science Distributed Active Archive Center for year 2007.

3.1 Rayleigh and surface reflectance

Atmospheric path radiance is composed of Rayleigh and aerosol radiances. The determination of Rayleigh path radiance is based on the computation of spectral dependence of the Rayleigh optical depth and phase function. The Bucholtz[12] equation (eq. (2)) was adopted for calculating the Rayleigh scattering optical thickness.

$$\tau_{\text{Ray}}(\lambda) = A \cdot \lambda^{-(B+C\lambda+D/\lambda)} \times \frac{p(z)}{p_0}, \quad (2)$$

where A, B, C, D are the constants of the total Rayleigh scattering cross-section and the total Rayleigh volume scattering coefficient at standard atmosphere. $P(z)$ is the pressure relevant to the height, which was determined by the parameterized barometric equation.

$$p(z) = p_0 \cdot \exp\left[\frac{-29.87 \cdot g \cdot 0.75 \cdot z}{8.315 \cdot (T_{\text{Surf}} - g \cdot 0.75 \cdot z)}\right]. \quad (3)$$

A fine resolution Digital Elevation Model (DEM) was used for estimating the height z and for calculating the

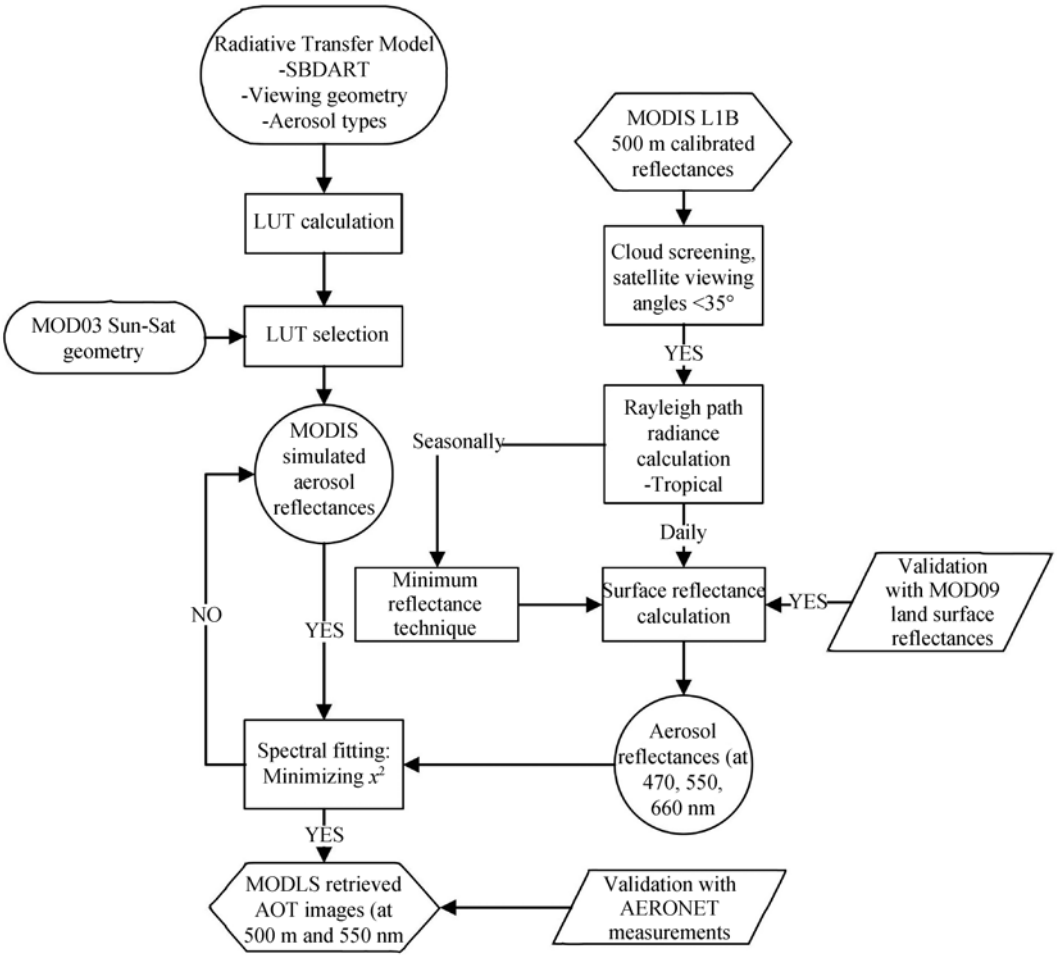

Figure 2 Schematic diagram for aerosol retrieval in the study.

pressure $p(z)$ for each pixel. g is the gravity acceleration (9.807 m/s^2) and T_{Surf} is the surface temperature.

The basic scheme of the modified MRT is to extract the minimum reflectance values of land surfaces over a period. To minimize seasonal land cover changes, seasonal minimum reflectance images were derived based on at least thirty clear-sky images for each of four seasons. Then, the second minimum reflectance values (rather than the actual minimum) were retrieved in order to avoid abnormal low reflectance such as noise or shadow. It was noted that the second minimum reflectance values have a stronger agreement with the surface reflectance. In addition, clouds were removed by thresholding the thermal waveband, which is essential in cloud-prone areas like Hong Kong. Only nadir images with satellite viewing angle <35^o have been considered in this study in order to minimize the angular effects caused by bidirectional reflectivity in heterogeneous areas.

3.2 Aerosol retrieval

The satellite measured aerosol reflectance decomposing from TOA reflectance, surface reflectance and Rayleigh path radiance can be fitted to values calculated from known aerosol optical properties to derive the AOT from the image wavelengths. This study adopted the Santa Barbara DISORT Radiative Transfer (SBDART; Ricchiazzi et al.[13]) model for constructing the LUT. Cluster analysis was used to classify natural and anthropogenic aerosols using 24 parameters from the AERONET aerosol and inversion products, which includes AOT (τ_{500}), angstrom exponent ($\alpha_{870-440}$), 4 single scattering albedo, 8 real and imaginary refractive index, 4 asymmetry factor, 2 mean radius, 2 standard deviation and 2 mode total volume. Four aerosol types were classified using 730 cases from 2005 to 2008. They are: i. mixed urban, ii. polluted urban, iii. dust, and iv. heavy pollution. Table 1 shows the aerosol and microphysical properties, as well as the number of records of each cluster.

For the results of clustering, type 1 (mixed urban aerosol) has the largest number (45% of total) and type 3 (dust) has the least number of records (3% of total). This reveals that the Hong Kong AERONET station is more exposed to urban pollution and only a few observations from desert dust from mainland China. Observations of desert dust may be limited by AERONET located within the urban area and the topographic effect caused by the high mountains and high rise buildings. Heavy urban pollution (type 4) accounts for 22% of total records, and type 2 (polluted urban aerosol) accounts for 30% of total records. In this classification, there is no clustering of rural and background aerosols types in Hong Kong.

Type 1 has the moderate absorption properties (SSA at 0.44 μm = 0.88) and it is dominated by both coarse and fine particles (Figure 3). Coarse mode most likely originates from sea salt and the fine mode most likely from local urban pollutants. In the existence of these two aerosol types, the absorbing properties could be determined by mixing state of carbonaceous particles. Since the AERONET is located 1 km from the coast, the sea salt and local urban pollutant are likely to be mixed; thus we refer to this type as mixed urban aerosol. Type 2 has the strongest absorption properties (SSA at 440 nm=0.87) and a high volume of fine particles (0.081). Small black carbon particles show high absorption properties. In Figure 3, type 2 and type 4 show similar size distribution but the former has lower AOT (0.52). We refer to this type as polluted urban aerosol. Dust (type 3) explains relative high AOT (τ_{500} = 0.51) with a large amount of coarse particles (68% of total volume concentration). Heavy pollution (type 4) is characterized by heavy aerosols (τ_{500} >1) and a large volume of fine particles (70%). The lower absorbing properties of heavy pollution could be explained by the mixture of particle types such as very small carbonaceous and sulfate particles.

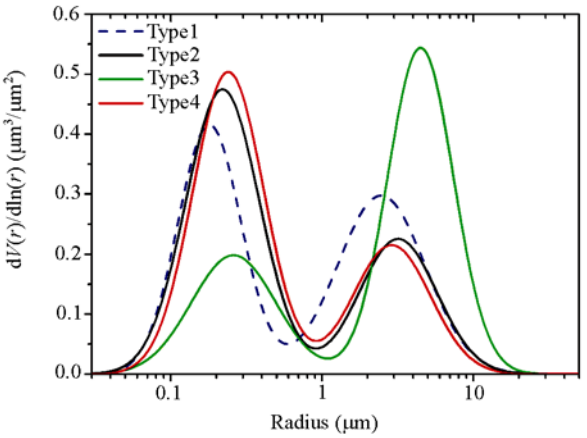

Figure 3 Aerosol size distributions used in this study.

For the LUT construction, the above 4 aerosol models with 9 solar zenith angles (0°~80°, Δ=10°), 17 view zenith angles (0°~80°, Δ=5°), 18 relative sun/satellite azimuth angles (0°~170°, Δ=10°) were considered. The SBDART code uses the aerosol properties associated with a given model, and the combinations of values for the 3 parameters listed above (amounting to 33048

Table 1 Summary of the cluster analysis results

	Type 1	Type 2	Type 3	Type 4
Aerosol optical thickness (500 nm)	0.451	0.518	0.510	1.065
Single scattering albedo (439 nm)	0.876	0.869	0.885	0.894
Single scattering albedo (676 nm)	0.889	0.874	0.871	0.911
Single scattering albedo (869 nm)	0.878	0.857	0.855	0.899
Single scattering albedo (1020 nm)	0.872	0.844	0.848	0.888
Real refractive index (676 nm)	1.470	1.452	1.500	1.452
Imaginary refractive index (676 nm)	0.014	0.022	0.016	0.015
Angstrom coefficient (870 nm/440 nm)	1.363	1.316	0.952	1.286
Asymmetry factor (676 nm)	0.643	0.665	0.683	0.682
Fine total volume	0.064	0.081	0.070	0.155
Fine mean radius	0.181	0.222	0.262	0.244
Geometric standard deviation (fine)	0.478	0.562	0.644	0.542
Coarse total volume	0.055	0.038	0.148	0.066
Coarse mean radius	2.458	3.177	4.484	2.892
Geometric standard deviation (coarse)	0.672	0.592	0.504	0.594
Number of records	332	216	22	160

combinations for 3 bands (470, 550, 660 nm)), to compute the hypothetical AOT. Figure 4 represents one of the LUTs from the SBDART results.

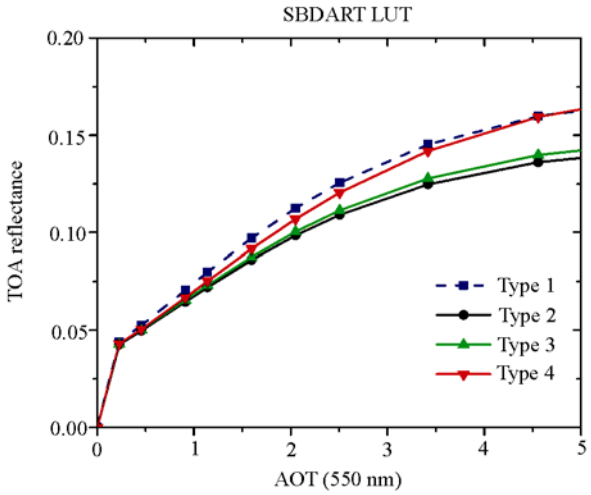

Figure 4 TOA reflectance as a function of AOT. The SBDART calculations were performed with solar zenith angle=30°, satellite zenith angle=10°, azimuth angle=150°.

The first step is the interpolation of the LUT geometry to the measured (satellite) geometry. This can reduce the number of LUT values being read in the computer memory. In the second step, hypothetical aerosol reflectance is determined based on the satellite estimated aerosol reflectance for the 470 nm band. Finally, the satellite observed aerosol reflectance is compared to the set of hypothetical aerosol reflectance for each geometrically-corrected LUT. For these comparisons, an optimal spectral shape-fitting technique was executed to select the aerosol model with the smallest systematic errors[1,14−16] (eq. (4)):

$$x^2 = \frac{1}{n}\sum_{i=1}^{n}\left(\frac{\rho_{\mathrm{Aer}}^{\mathrm{mea}}(\lambda_i)-\rho_{\mathrm{Aer}}^{\mathrm{mod}}(\lambda_i)}{\rho_{\mathrm{Aer}}^{\mathrm{mea}}(\lambda_i)}\right)^2. \quad (4)$$

The error term of x^2 is described as the residual of the measured aerosol reflectance $\rho_{\mathrm{Aer}}^{\mathrm{mea}}(\lambda_i)$ from MODIS and modeled aerosol reflectance $\rho_{\mathrm{Aer}}^{\mathrm{mod}}(\lambda_i)$ from aerosol models, $n=3$ (3 wavelengths). The minimum residual of x^2 is selected from the four aerosol types for each pixel. Thus, the appropriate aerosol type is selected and the corresponding AOT values are then derived for each pixel.

4 Result

4.1 Validation with surface reflectance

The minimum reflectance images have been derived seasonally for the estimation of surface reflectance (Figure 5). Validation of the MRT images was undertaken by comparing with the MODIS surface reflectance products (MOD09: 8-days composite surface reflectance images). The MOD09 images are corrected for aerosol, gaseous and water vapor using the inputs of MODIS atmospheric data. Strong correlations were observed in the fall and winter seasons (r>0.9), whereas moderate correlations were noted in the spring season (r>0.8) (Table 2). The differences in surface reflectance (y-intercepts of the slopes) were less than or equal to 0.01 for the 550 and 660 nm wavelengths whereas the differences are greater for the shorter 470 nm wavelength

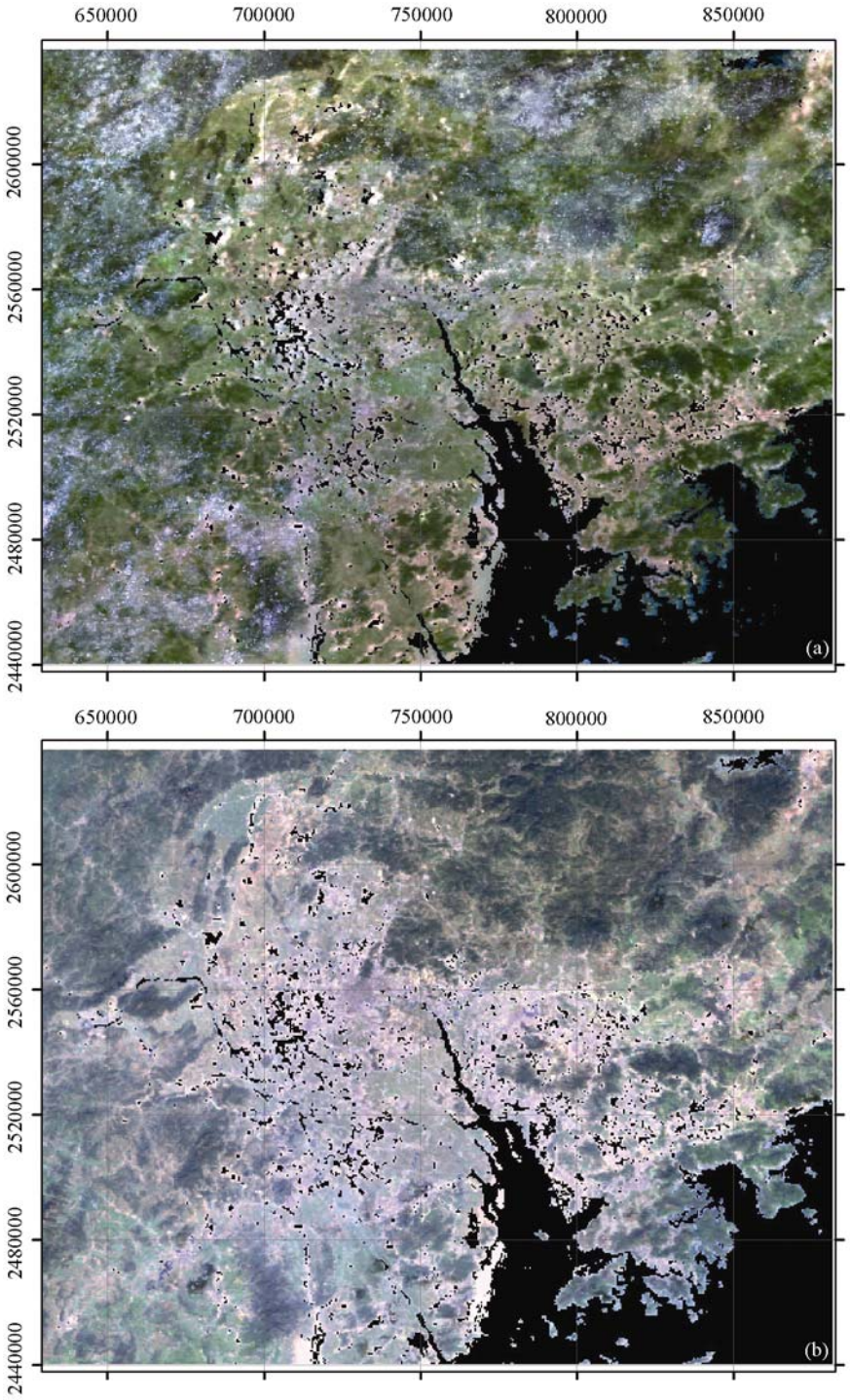

Figure 5 Surface reflectance maps in fall season. (a) RGB composite of MOD09. (b) RGB composite of MRT.

Table 2 Summary of correlations (r) between surface reflectance derived from MRT and from MOD09 products

Wavelength	470 nm	550 nm	660 nm
Spring	0.870	0.902	0.937
Autumn	0.947	0.950	0.940
Winter	0.938	0.933	0.943

(~0.02－0.03).

4.2 Validation with AERONET measurements

The MODIS 500 m retrieved AOT was validated using AERONET measurements (Figure 6(a)) and a good agreement is shown between our methodology and the AERONET, with a correlation coefficient r=0.891. For further comparison, the MOD04 collection 4 and 5 AOT data at 10 km resolution were also compared with AERONET (Figure 6(b)). The correlation coefficients of r=0.913 and r=0.877 were observed from collection 5 and collection 4 respectively. The correlation coefficient of our methodology is in between the values of collection 5 and 4, but it has a smaller magnitude of underestimation of AOT (~0.025) than that of collection 4 and 5. Most importantly, our methodology can retrieve AOT images at a much higher spatial resolution, and thus can show detailed AOT levels over both bright urban and dark rural vegetated areas. This improvement is significant for a topographically complex area like Hong Kong.

4.3 Applications

The AOT distribution over Hong Kong and the PRD region on 28 January 2007 and 30 January 2007 retrieved using MODIS 500 m data are shown in Figure 7(a), (b). The overall AOT of 28 January 2007 is relatively low with a range of ~0.4 in rural areas to ~1.4 in urban areas. It is particularly notable that in industrialized areas of the PRD e.g., Guangzhou city and Shunde district, high AOT is observed due to anthropogenic pollution sources. However the general AOT of Hong Kong on the same date is comparatively low ~0.6. A rapid increase of AOT occurred two days later on 30 January 2007. This extremely high AOT (~1.8) was observed over most industrialized areas in the PRD and it is shown as red color in Figure 7(b). There are many industries and power plants located there and due to the low wind speeds (~1.5 m/s) on that day, the air pollutants would be trapped in the PRD region. The northern part of Hong Kong, especially near the Chinese city of Shenzhen, commonly suffers from cross-boundary pollutants which are emitted from industries in the PRD region, and here AOT values of 1.0 are observed on 30 January 2007. The MODIS collection 5 AOT image is visually and spatially inferior due to its coarser resolution (10 km) and is ineffective for aerosol mapping in urban areas. The rapid changes of aerosol contents over the PRD region and Hong Kong can be monitored using our methodology with higher resolution and it is easier to pinpoint the sources of anthropogenic emission.

5 Conclusion

This study demonstrates a new aerosol retrieval algorithm for MODIS 500 m data based on a modified MRT to derive surface reflectance images coupled with comprehensive LUTs, which consider different aerosol models derived from Hong Kong AERONET measurements and sun-satellite geometries in radiative transfer modeling. The MODIS 500 m AOT is able to estimate aerosols over both urban and vegetated areas at a high level of detail. A good correlation was found between land sur-

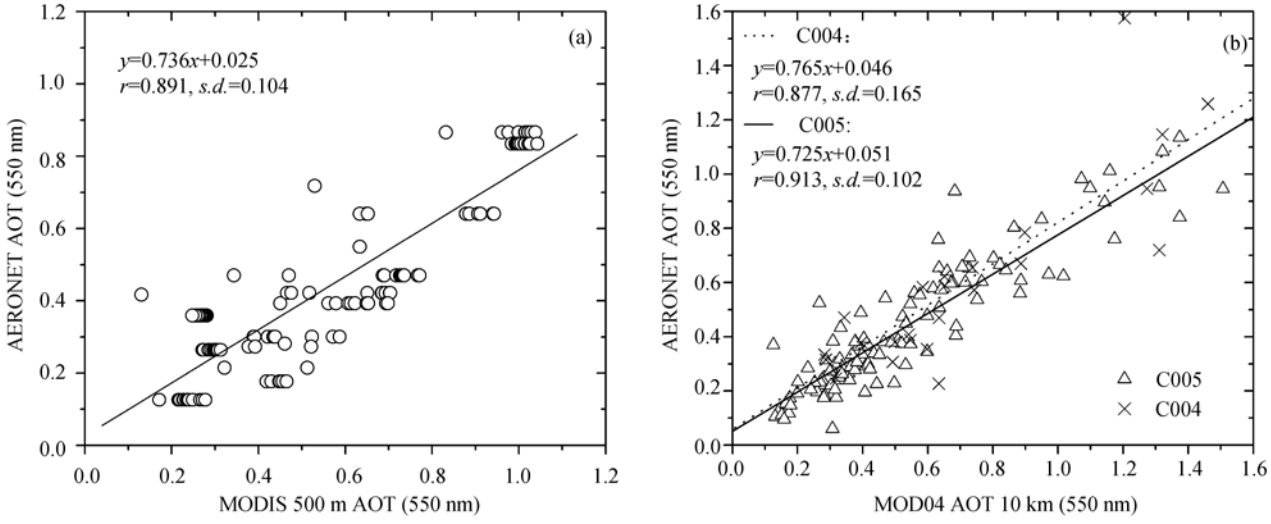

Figure 6 (a) Scatter plots between MODIS 500 m AOT with AERONET measurements; (b) Scatter plots between MOD04 collection 4 and 5 AOT with AERONET measurements.

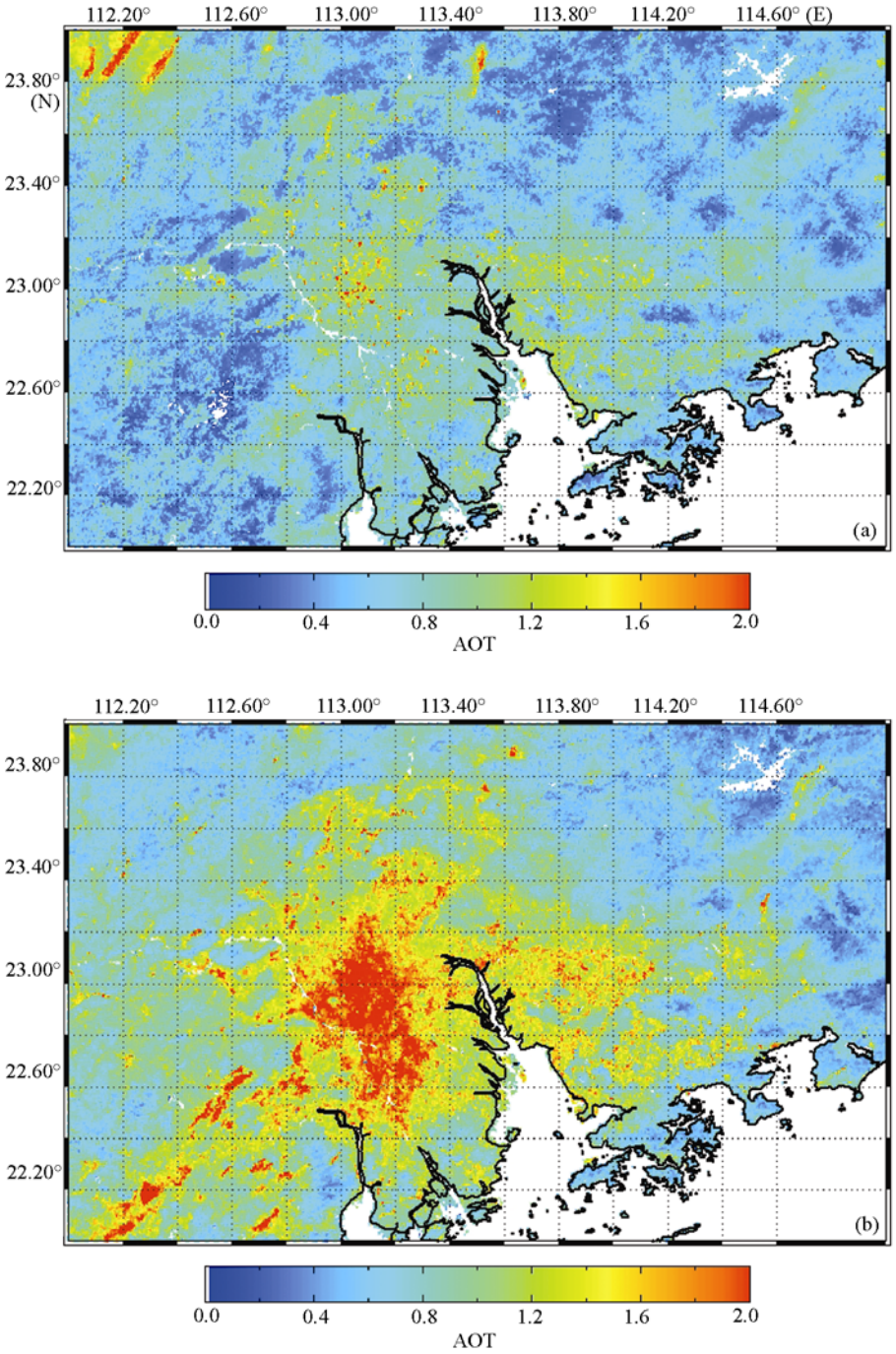

Figure 7 AOT at 550 nm with 500 m resolution over Hong Kong and the Pearl River Delta (PRD) region on 28 January 2007 (a) and 30 January 2007 (b).

face reflectance from MOD09 products and the MRT images, and this suggests the MRT images are useful for estimation of surface reflectance. The derived MODIS 500 m AOT shows a high level of accuracy (r=0.891) compared with ground-based AERONET measurements. The results are also comparable with MODIS collection 4 and collection 5 data, with r=0.877 and r=0.913. Although the collection 5 performs a slightly higher correlation than our method, its spatial inferiority due to coarse resolution limits its application in urban areas. Given the high accuracy and higher spatial resolution of the derived MODIS 500 m AOT images, they can be used to study transient cross-boundary aerosols and localized intra-urban aerosol distributions.

We thank the NASA Goddard Earth Science Distributed Active Archive Center for the MODIS Level IB and Level 2 data, and Brent Holben for help with the Hong Kong PolyU AERONET station.

1 Kaufman Y J, Tanré D. Algorithm for Remote Sensing of Tropospheric Aerosol from MODIS. NASA MOD04 Product ATBD Report, 1998

2 Chu A, Kaufman Y J, Ichoku C, et al. Validation of MODIS aerosol optical depth retrieval over land. Geophys Res Lett, 2002, 29(12): 1－4

3 Holben B N, Eck T F, Slutsker I, et al. AERONET－A federated instrument network and data archive for aerosol characterization. Remote Sens Environ, 1998, 66(1): 1－16

4 Remer L A, Kaufman Y J, Tanré D, et al. The MODIS aerosol algorithm, products and validation. J Atmos Sci, 2005, 62(4): 947－973

5 Levy R C, Remer L A, Martins J V, et al. Evaluation of the MODIS aerosol retrievals over ocean and land during CLAMS. J Atmos Sci, 2004, 62(4): 974－992

6 Levy R C, Remer L A, Mattoo S, et al. Second-generation operational algorithm: Retrieval of aerosol properties over land from inversion of Moderate Resolution Imaging Spectroradiometer spectral reflectance. J Geophys Res, 2007, D13211: 112

7 Mi W, Li Z Q, Xia X G, et al. Evaluation of the MODIS aerosol products at two AERONET stations in China. J Geophys Res, 2007, D22S08: 112

8 Herman J R, Celarier E A. Earth surface reflectivity climatology at 340－380 nm from TOMS data. J Geophys Res, 1997, 102: 28003－28011

9 Koelemeijer R B A, de Haan J F, Stammes P. A database of spectral surface reflectivity in the range 335–772 nm derived from 5.5 years of GOME observations. J Geophys Res, 2003, 108: 28003－28011

10 Li C C, Lau A K H, Mao J T, et al. Retrieval, validation, and application of the 1-km aerosol optical depth from MODIS measurements over Hong Kong. IEEE Trans Geosci Remote Sensing, 2005, 43(11): 2650－2658

11 CH2M HILL (China) Limited. CH2M Study of Air Quality in the Pearl River Delta Region, Final Report, R0355.01. Environmental Protection Department, The Government of Hong Kong Special Administrative Region, 2002

12 Bucholtz A. Rayleigh-scattering calculations for the terrestrial atmosphere. Appl Optics, 1995, 34: 2765－2773

13 Ricchiazzi P, Yang S R, Gautier C, et al. SBDART: A research and teaching software tool for plane-parallel radiative transfer in the Earth's atmosphere. Bull Amer Meteorol Soc, 1998, 79(10): 2101－2114

14 Costa M J, Cervino M, Cattani E, et al. Aerosol optical thickness and classification: Use of METEOSAT, GOME and modeled data. In: Russell J E, ed. EOS-Spie International Symposium on Remote Sensing. Satellite Remote Sensing of Clouds and the Atmosphere IV. Proc SPIE, 1999, 3867: 268－279

15 Torricella F, Cattani E, Cervino M, et al. Retrieval of aerosol properties over the ocean using global ozone monitoring experiment measurements: Method and applications to test cases. J Geophys Res, 1999, 104(10): 12085－12098

16 Lee K H, Kim Y J, von Hoyningen-Huene W, et al. Spatio-temporal variability of atmospheric aerosol from MODIS data over Northeast Asia in 2004. Atmos Environ, 2007, 41(19): 3959－3973